AD_____

Award Number: W81XWH-08-1-0192

TITLE: INCORPORATING FUNCTIONAL IMAGING INFORMATION TO rpFNA ANALYSIS FOR BREAST CANCER DETECTION IN HIGH-RISK WOMEN

PRINCIPAL INVESTIGATOR: KRISTY L. PEREZ

CONTRACTING ORGANIZATION: Duke University
Durham, NC 27706

REPORT DATE: March 2011

TYPE OF REPORT: Annual Summary

PREPARED FOR: U.S. Army Medical Research and Materiel Command
Fort Detrick, Maryland 21702-5012

REPORT DOCUMENTATION PAGE

Form Approved
OMB No. 0704-0188

1. REPORT DATE *(DD-MM-YYYY)*	**2. REPORT TYPE**	**3. DATES COVERED** *(From - To)*
01-03-2011	Annual Summary	1 MAR 2008 - 28 FEB 2011

4. TITLE AND SUBTITLE
INCORPORATING FUNCTIONAL IMAGING INFORMATION TO rpFNA ANALYSIS FOR BREAST CANCER DETECTION IN HIGH-RISK WOMEN

5a. CONTRACT NUMBER

5b. GRANT NUMBER
W81XWH-08-1-0192

5c. PROGRAM ELEMENT NUMBER

6. AUTHOR(S)
KRISTY L. PEREZ

E-Mail: kristy.perez@duke.edu

5d. PROJECT NUMBER

5e. TASK NUMBER

5f. WORK UNIT NUMBER

7. PERFORMING ORGANIZATION NAME(S) AND ADDRESS(ES)
Duke University
Durham, NC 27706

8. PERFORMING ORGANIZATION REPORT NUMBER

9. SPONSORING / MONITORING AGENCY NAME(S) AND ADDRESS(ES)
U.S. Army Medical Research and Materiel Command
Fort Detrick, Maryland 21702-5012

10. SPONSOR/MONITOR'S ACRONYM(S)

11. SPONSOR/MONITOR'S REPORT NUMBER(S)

12. DISTRIBUTION / AVAILABILITY STATEMENT
Approved for Public Release; Distribution Unlimited

13. SUPPLEMENTARY NOTES

14. ABSTRACT

The overall goal of this work is to correlate the imaging information from the dual-modality, dedicated single photon emission computed tomography (SPECT) and computed tomography device with the results of random periareolar fine needle aspiration (rpFNA) in women at high risk for breast cancer. In this third year of work, the variability of the quantification procedure has been evaluated with the Two One-Sided Test. The SPECT images can be statistically significantly quantified within ±10% of known values when acquired with traditional trajectories. The SPECT image quantification acquired with non-traditional trajectories has borderline p-values that are nearly statistically significant (p=0.052). Quantification was retrospectively applied to human subject data and it was determined that more information about the normal radiotracer uptake should be acquired. Work resulting from this project was presented at a local seminar and international conference this year and several manuscripts are being submitted for peer review.

15. SUBJECT TERMS
Nuclear Medicine Imaging, SPECT, Molecular Breast Imaging, Mammotomography, rpFNA

16. SECURITY CLASSIFICATION OF:			**17. LIMITATION OF ABSTRACT**	**18. NUMBER OF PAGES**	**19a. NAME OF RESPONSIBLE PERSON**
a. REPORT	**b. ABSTRACT**	**c. THIS PAGE**			USAMRMC
U	U	U	UU	19	**19b. TELEPHONE NUMBER** *(include area code)*

Table of Contents

A. Introduction

The overall goal of this work was to correlate the imaging information from our dual-modality, dedicated single photon emission computed tomography (SPECT) and computed tomography (CT) device with results of random periareolar fine needle aspiration (rpFNA) in women at high risk for breast cancer. The quantitative functional imaging signal from the whole breast could differentiate between normal and abnormal tissues, but first the normal uptake of the ^{99m}Tc-sestamibi radiotracer must be established. In this third year of work, the quantification procedure has been evaluated with two one-sided test (TOST) analysis to determine if the quantitative functional imaging signal is statistically equivalent to the known activity concentration. I have additionally fulfilled other aspects of the training program, including attending local and international conferences, submitting papers for peer review and preparing the PhD dissertation and defense.

B. Body

The Statement of Work and proposed timeline are included in Appendix A. For Year 3, the tasks outlined preparations for and initiation of collecting human subject SPECT-CT images of women who are undergoing ^{99m}Tc-sestamibi imaging for parathyroid disease. These breast images will provide information about range of activity concentration in normal, asymptomatic breast tissue that will ultimately determine whether or not to proceed with injecting ^{99m}Tc into high risk women and correlating the breast image signal with rpFNA data. The SPECT signal quantification is within ± 10% of the known quantity.

Task 1: Acquire IRB approval

Task 1(a): Participate on writing IRB protocol for FMT imaging in a high risk patient cohort.

Based on the findings of this research, it has been decided that the range of ^{99m}Tc-sestamibi activity concentrations in normal breast tissue of asymptomatic women should be measured to have as a comparison before imaging the high risk patient cohort. The ^{99m}Tc-sestamibi radiotracer is currently used at Duke University Medical Center for imaging parathyroid disease, which is not correlated with breast cancer. The mostly female parathyroid patients are imaged immediately after injection for 10min and then again 2 hours after injection, where between the two scans they remain in the Nuclear Medicine waiting room. An Institutional Review Board (IRB) protocol has been approved to recruit and image female parathyroid patients during the time between their nuclear medicine imaging studies. Because these women will have already been injected with the radiotracer, the additional risk to the women is only the x-ray dose from the computed tomography (CT) acquisition. One major complication that led to only very recently obtaining IRB approval utilizing our NIH developed SPECT-CT device is that the Duke IRB now required an FDA abbreviated-IDE approval prior to allowing the IRB protocol. Unfortunately for this grant project, this approval has come too late to acquire human subjects. Nonetheless, the MMI Lab will continue to acquire that baseline breast uptake information for future studies.

Task 3: Optimize patient imaging and biopsy protocol.

Task 3(b): Investigate how the information gained with SPECT imaging can be incorporated into the biopsy procedure

The variability of the quantification procedure was investigated by repeatedly imaging an anthropomorphic breast phantom filled with ^{99m}Tc-pertechnetate (Figure 1). Activity in the phantom was filled each day at a concentration 10 times greater than that expected clinically, approximately 0.39 μCi/mL [1]. For vertical axis of rotation (VAOR), tilted parallel beam (TPB) and projected sinusoidal wave (PROJSINE) trajectories [2], 5 sequential data sets were collected, each containing 128 projections with a ±4% energy window. After ~18 hours (3 half lives), 5 sequential data sets were again collected of the stationary phantom using the same trajectories and acquisition parameters from the previous day to obtain images at clinical activity concentration (~0.047 μCi/mL). The same phantom setup with similar amounts of activity was imaged on 3 occasions after applying a new uniformity correction and acquiring a point source to determine the reconstruction scaling factor.

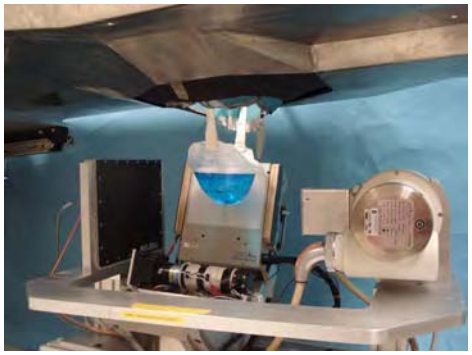

Figure 1: Photograph of the water-filled, 700mL breast phantom hanging in the FOV of the SPECT-CT system.

Attenuation and scatter correction [3, 4] was applied to these data sets, and each data set was reconstructed with the OSEM algorithm [5] to the 20th iteration. The edge of the breast phantom in the SPECT image was aligned to the edge in a CT image. A volume of interest (VOI) was created with the whole volume of the CT image and applied to the SPECT image (Figure 2). The mean value in the VOI in each image for the two activity concentrations was compared to the "known" dose calibrator value. The TOST compared the mean activity concentration in the breast phantom VOI for each image acquisition with the dose calibrator measurement. The statistical tests were carried out with two acceptable difference values: one derived from the error in the dose calibrator measurement and the other set at 10% of the known activity concentration.

The reconstructed data is noisy, especially for the images with clinical activity concentration, due to the low count rates (Figure 3). The noise in these images looks like what a suspicious area would look like when detecting breast cancer (white and yellow spots in images). In the images of the breast phantoms at clinical activity concentrations, the edge of the breast phantom is not clear, and there are regions where there appears to be no activity (Figures 2 & 3), similar to what we have seen in human subject imaging.

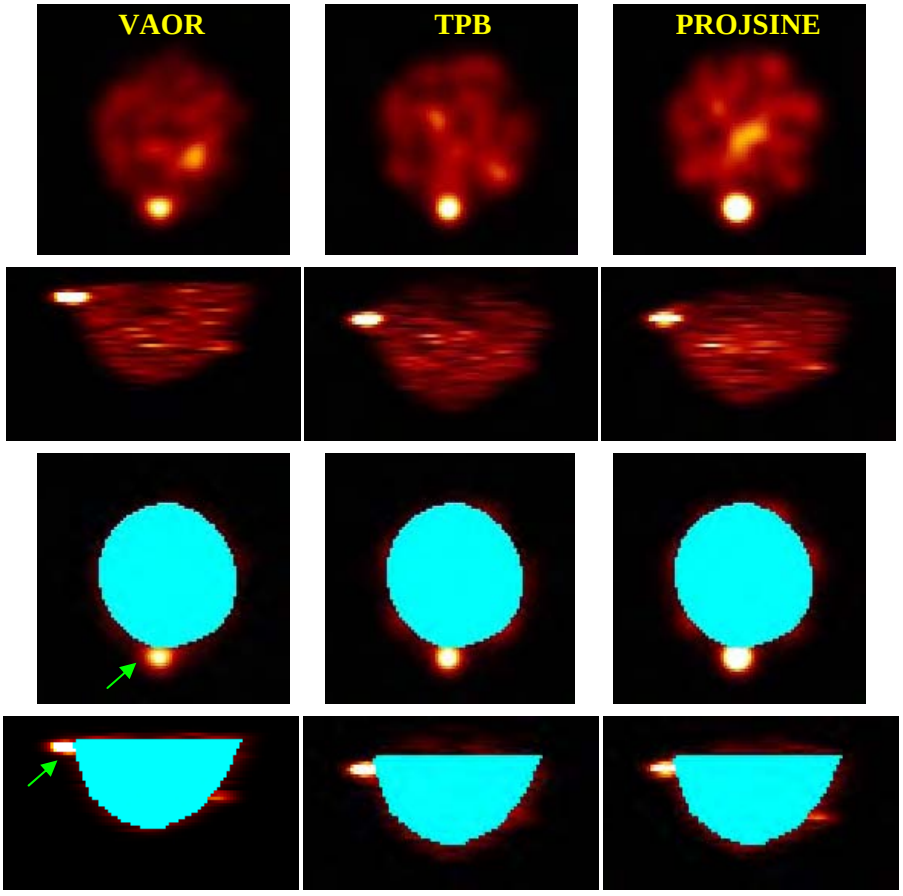

Figure 2: (ROW 1) Coronal and (ROW 2) transverse slices (smoothed with a Gaussian filter) of 10X clinical activity concentration (0.36 µCi/mL) images acquired on Day 1 with (LEFT) VAOR, (CENTER) TPB and (RIGHT) PROJSINE trajectories. (ROW 3) Coronal and (ROW 4) transverse slices (smoothed with a Gaussian filter) showing the placement and size of the VOI used to measure the average activity concentration in the phantoms derived from a CT image acquired of the breast phantom. Fiducial markers (green arrows) demonstrate that the VOI was within the bounds of the breast phantom.

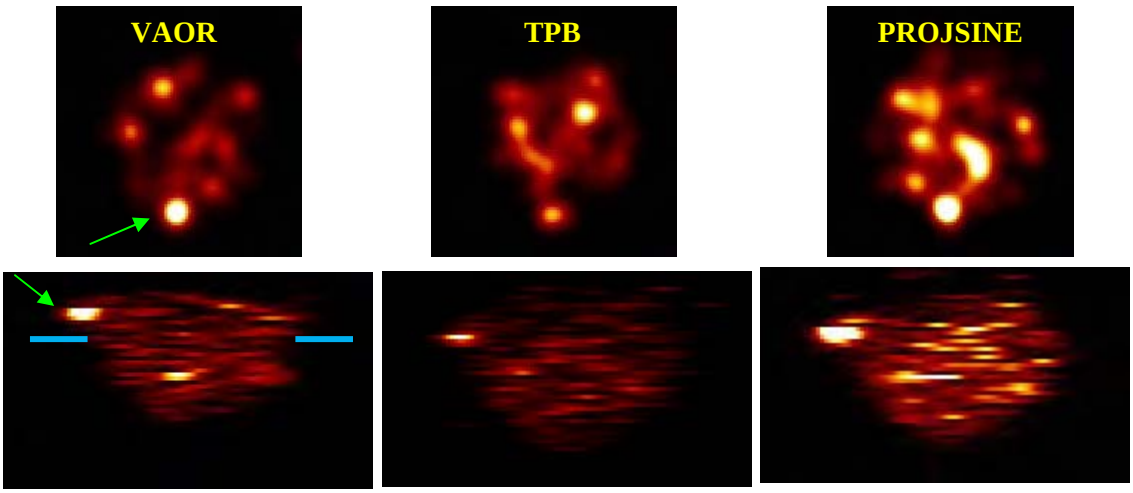

Figure 3: (TOP) Coronal and (BOTTOM) transverse slices (smoothed with a Gaussian filter) of clinical activity concentration (0.047 µCi/mL) images acquired on Day 1 with (LEFT) VAOR, (CENTER) TPB and (RIGHT) PROJSINE trajectories. Aqua lines in the transverse image indicate the location of the coronal slice. Green arrows point to fiducial markers attached to the outside of the breast.

When the acceptable difference is determined by the error propagation from the dose calibrator and volume measurements, the image-based measured values are not equivalent to the known values in any case (Tables 1 & 2). However, for the attenuation- and scatter-corrected data, the images acquired at 10X clinical count rates are statistically equivalent to within ±10% of the known value for each trajectory (Table 1). At the clinical count rates of the attenuation- and scatter-corrected data, the VAOR data is statistically equivalent to within ±10% of the known value, but neither the TPB nor the PROJSINE data are (Table 2). The PROJSINE data is borderline and would very likely be statistically equivalent if the acceptable difference was relaxed to ±15%.

Table 1: The actual difference and p-values for the TOST with the acceptable difference based on the error of the dose calibrator measurement (0.022 µCi/mL) and based on ±10% of the dose calibrator measurement (0.036 µCi/mL) for the 10x clinical data.

Trajectory	Actual Difference	0.022 µCi/mL		0.036 µCi/mL	
		Upper p-value	Lower p-value	Upper p-value	Lower p-value
VAOR	0.018	0.22	<0.0001	0.0003	<0.0001
TPB	-0.027	<0.0001	0.85	<0.0001	0.039
PROJSINE	-0.024	<0.0001	0.70	<0.0001	0.0018

Table 2: The actual difference and p-values for the TOST with the acceptable difference based on the error of the dose calibrator measurement (0.0029 µCi/mL), and based on ±10% of the dose calibrator measurement (0.0047 µCi/mL) for the clinical data.

Trajectory	Actual Difference	0.0029 µCi/mL		0.0047 µCi/mL	
		Upper p-value	Lower p-value	Upper p-value	Lower p-value
VAOR	0.0027	0.42	<0.001	0.016	<0.0001
TPB	-0.0041	<0.0001	0.87	<0.001	0.31
PROJSINE	-0.0031	<0.0001	0.59	<0.001	0.052

Using the maximum volume imaged of the breast will give the best average activity concentration and is appropriate for measuring normal asymptomatic breasts. However, smaller VOIs will need to be used to measure breasts with abnormal tissue. These smaller VOI measurements may be affected by systematic spatial variation due to the nature of the non-traditional acquisition trajectories. To determine if the accuracy of the activity

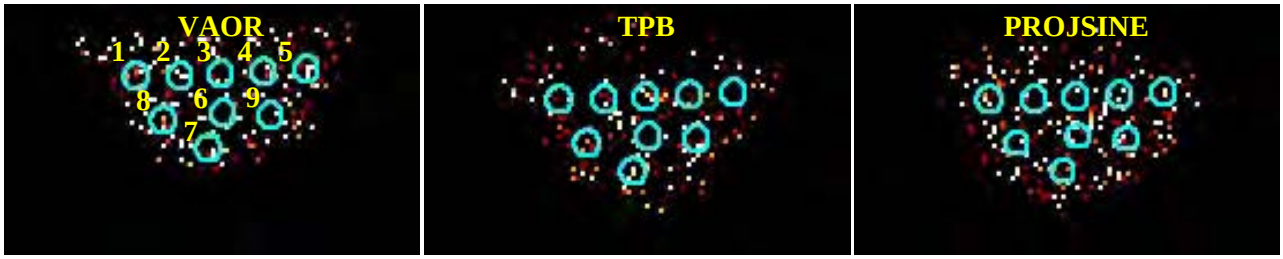

Figure 4: Transverse slices through (LEFT) VAOR, (CENTER) TPB and (RIGHT) PROJSINE 10X clinical images of the breast phantom showing the placement of the nine 15mm diameter spherical VOIs throughout the breast.

quantification varies over the volume of the breast, nine 15mm diameter spherical VOIs were drawn throughout the breast volume (Figure 4) in images acquired with each trajectory on day 1 only (5 scans for each trajectory). To elucidate a dependence on location, the mean of the small VOI was divided by the mean of the whole breast VOI for each scan; this ratio should equal one if there is no dependence on location. Then, the average and standard deviation of the 5 ratios for the respective acquisition trajectory were calculated. Comparisons were made between the ratios throughout the breast volume to determine how the activity concentration quantification varies.

The analysis for the VAOR acquired data at 10X clinical activity concentration shows data trends downward toward the center of the breast (Figure 5 TOP, Regions 1 through 5) and upward from the chest wall to the nipple (Figure 5 TOP, Regions 3, 6 and 7). However in the TPB and PROJSINE data, the ratio of the mean activity concentration in the small VOI to the whole breast VOI are equal within one standard deviation. At the clinical activity concentration, all the ratios of the mean activity concentrations are equal to within one standard deviation across the width of the breast (Regions 1 through 5) for each trajectory, except for the VAOR data in Region 1, (Figure 5, BOTTOM). Additionally, from the chest wall to the nipple (Regions 3, 6 and 7), the PROJSINE and TBP trajectories have ratios of the mean activity concentrations equal to one standard deviation, but the VAOR data are not equal and there is no trend. At both 10X clinical and clinical activity concentrations, the middle of the length of the breast (Regions 6, 8 and 9) are equal within one standard deviation for each trajectory. The average over the nine regions for each trajectory at each concentration equals approximately one, the expected value. The trends in the VAOR data are unexpected because applying attenuation and scatter corrections should result in homogeneous activity distribution for this fully sampled breast phantom. The TPB and PROJSINE trajectories are not fully sampled, yet have no location dependent difference in the mean activity concentration measurement. One caveat is these data may not have sufficient count statistics to elucidate systematic errors because the data were acquired to determine if the quantification procedure produce image signals within an acceptable difference of the dose calibrator for human imaging. This study of smaller VOIs should be repeated with increased count statistics to better determine any spatial variations.

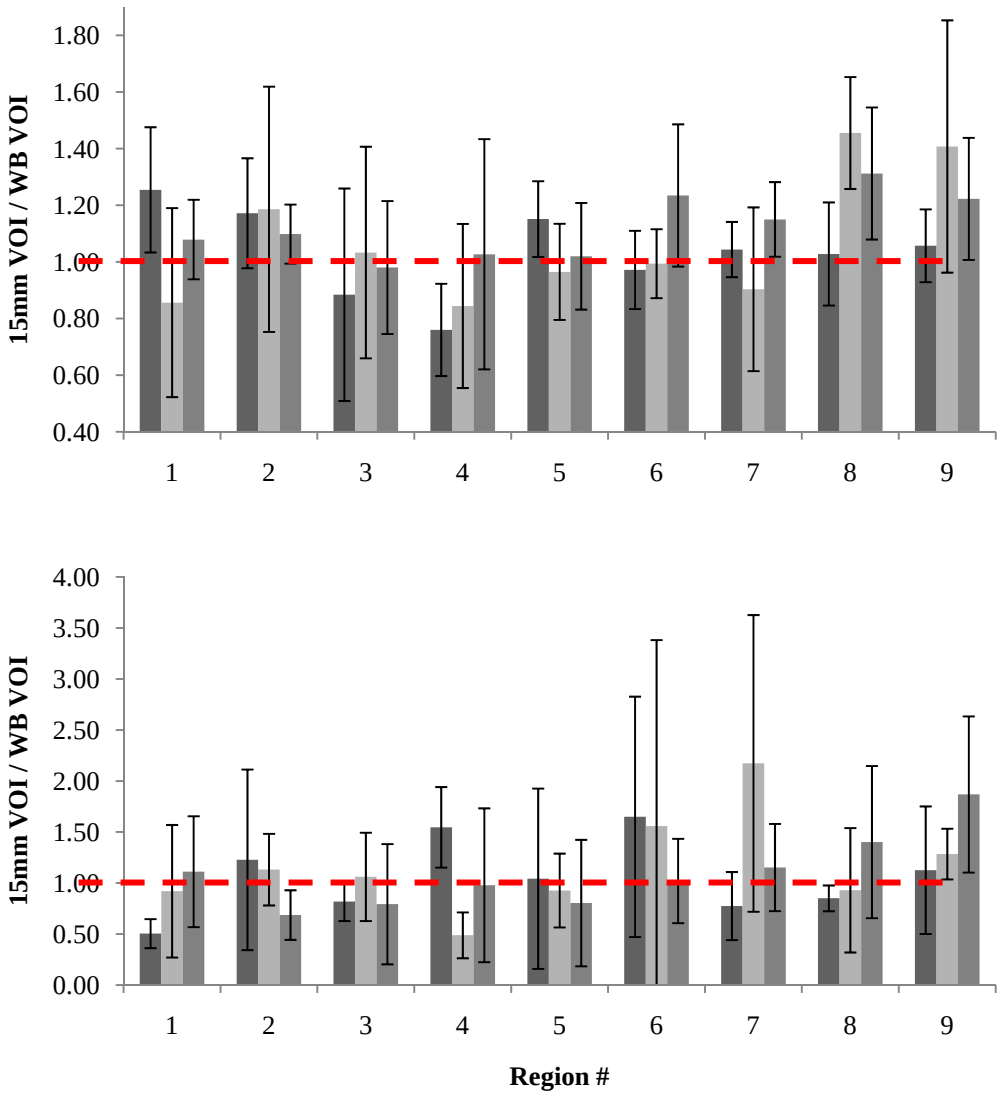

Figure 5: The ratio of the 15mm diameter VOI compared to the whole breast VOI in the (TOP) 10X clinical and (BOTTOM) clinical activity concentration images acquired with (■) VAOR, (■) TPB and (■) PROJSINE trajectories. The red dotted line represents the small VOI to whole breast VOI ratio of one.

Task 4: Complete other aspects of breast cancer training program

Task 4(b): Publish research work in peer-reviewed journals

In July 2010, "Characterizing the contribution of cardiac and hepatic uptake in dedicated breast SPECT using tilted trajectories" was published in *Physics in Medicine and Biology* [6]. A manuscript, "Towards quantification of functional breast images using dedicated SPECT with non-traditional trajectories," has been accepted with revisions to *IEEE Transaction on Nuclear Science*.

Task 4(d): Attend international conferences

I attended and gave a poster presentation at 2010 *Society of Nuclear Medicine Annual Meeting* in Salt Lake City, Utah (see Reportable Outcomes). Additionally, a co-author presented a poster presentation at the *IEEE Nuclear Science Symposium and Medical Imaging Conference* in Knoxville, TN in October 2010 (see Reportable Outcomes).

Task 4(e): Prepare and defend thesis

I have written and submitted my dissertation to my committee entitled "Investigating Functional Breast Image Quality and Quantification with a Dedicated Breast SPECT-CT System". I will be defending on April 4, 2011.

C. Key Research Accomplishments

Continuing progress on tasks 3-4 was made in Year 3. Tasks 1-3 have been investigated over the course of this 3 year grant period and the finding are as follows:

- Based on data obtained and analyzed during this grant period, it is recommended to acquire images of normal breast tissue from asymptomatic human subjects to have for comparison of the images of women at high risk for breast cancer.
- An IRB protocol has been approved for recruiting ^{99m}Tc-sestamibi parathyroid imaging patients, who are otherwise asymptomatic for breast disease, to have their breasts imaged with the dedicated SPECT-CT system.
- The activity concentration of ^{99m}Tc-sestamibi in normal tissue coupled with the dimensions of the rpFNA needle indicates that imaging the rpFNA needles after aspiration will not provide a distinct signal above system noise and therefore, this research path should not be further pursued at this time.
- The procedure to quantify the activity measured in SPECT images has been refined and tested.
- The variability of the whole breast activity concentration measurement has been investigated and compared to known quantities of activity. The procedure results in quantities within ±10% of the known value, an excellent result for nuclear medicine study.

D. Reportable Outcomes

Year 3

Peer Reviewed Publications

SJ Cutler, **KL Perez**, MP Tornai. "Observer Detection Limits for a Dedicated SPECT Breast Imaging System." *Phys. Med. Biol.*, **55**:1903-1916, 2010.

KL Perez, SJ Cutler, P Madhav, MP Tornai. "Characterizing the contribution of cardiac and hepatic uptake in dedicated breast SPECT using tilted trajectories." *Phys Med Biol*. 55(16): 4721-734, 2010.

In Review

KL Perez, SJ Cutler, P Madhav, MP Tornai. "Towards Quantification of Functional Breast Images using Dedicated SPECT with Non-Traditional Acquisition Trajectories." *IEEE Trans. Nucl. Sci. (Accepted for publication)*

Conference Proceedings

KL Perez, SD Mann, J Pachon, P Madhav, MP Tornai. "Is SPECT or CT Based Attenuation Correction More Quantitatively Accurate for Dedicated Breast SPECT Acquired with Non-Traditional Trajectories?" Presented at the *2010 IEEE Nucl. Scie Symposium & Med. Imaging Conference*, Knoxville, TN, 30 Oct. – 6 Nov. 2010, and published in *IEEE Conference Record NSS/MIC*.

Abstracts and Presentations

KL Perez, SJ Cutler, P Madhav, MP Tornai. "Whole breast quantification with dedicated SPECT-CT." Presented at the *2010 Society of Nuclear Medicine Meeting*, Salt Lake City, UT, 5-9 Jun. 2010, and published in J. Nucl. Med. 51(Supplement 2). 1350.

Year 1 & 2

Conference Proceedings

P Madhav, SJ Cutler, DJ Crotty, **KL Perez**, RL McKinley, PK Marcom, T Wong, MP Tornai. "Pilot Patient Studies Using a Dedicated Dual-Modality SPECT-CT System for Breast Imaging." Presented at the *50th Annual Meeting of the American Association of Physicists in Medicine*, Houston, TX, 27-31 Jul. 2008.

SJ Cutler, **KL Perez**, P Madhav, MP Tornai. "Comparison of 2D scintimammography and 3D dedicated breast SPECT using a compressible breast phantom and lesions of varying size and tracer uptake." Presented at the *2008 IEEE Fourth International Workshop on the Molecular Radiology of Breast Cancer*, Dresden, Germany, 20-21 Oct. 2008, and published in *IEEE Conference Record NSS/MIC*, 5640-5646.

DJ Crotty, SJ Cutler, P Madhav, **KL Perez**, RL McKinley, MP Tornai. "Improved Chest Wall Imaging through Combined Complex Trajectories in Dedicated Dual Modality SPECT-CT Breast Molecular Imaging." Presented at the *Fourth International Workshop on the Molecular Radiology of Breast Cancer (MRBC)*, Dresden, Germany, 20 - 21 Oct. 2008, and published in 2008 IEEE Medical Imaging Conference Record, 5650-5665.

KL Perez, SJ Cutler, P Madhav, MP Tornai "Novel Patient Acquisition Trajectories for Optimized Dedicated Breast SPECT Imaging." Presented at the *Fourth International Workshop on the Molecular Radiology of Breast Cancer (MRBC)*, Dresden, Germany, 20 - 21 Oct. 2008, and published in 2008 IEEE Medical Imaging Conference Record, 5629-5634.

KL Perez, SJ Cutler, P Madhav, MP Tornai. "Towards quantification of dedicated breast SPECT using non-traditional acquisition trajectories." Presented at the *2009 IEEE Nucl. Sci. Symposium & Med. Imaging Conference*, Orlando, FL, 25-31 Oct. 2009, and published in *IEEE Conference Record NSS/MIC*, 3866-3870.

KL Perez, SJ Cutler, P Madhav, MP Tornai. "Is SPECT or CT Based Attenuation Correction More Quantitatively Accurate for Dedicated Breast SPECT Acquired with Non-Traditional Trajectories." Presented at the *2010 IEEE Nucl. Sci. Symposium & Med. Imaging Conference*, Knoxville, TN, 30 Oct. – 6 Nov. 2010, and published in *IEEE Conference Record NSS/MIC*.

Abstracts and Presentations

DJ Crotty, P Madhav, SJ Cutler, **KL Perez**, RL McKinley, MP Tornai, "Performance of a new dual-modality molecular-anatomical imaging system dedicated to breast cancer." Presented at the *2008 Duke Cancer Center Annual Meeting*, Durham, NC, 10 Mar. 2008.

P Madhav, SJ Cutler, DJ Crotty, **KL Perez**, RL McKinley, PK Marcom, TZ Wong, MP Tornai. "Dedicated molecular and anatomical breast imaging - initial patient studies." Presented at the *2008 Duke Cancer Center Annual Meeting*, Durham, NC, 10 Mar. 2008.

P Madhav, SJ Cutler, DJ Crotty, **KL Perez**, RL McKinley, L Wilke, TZ Wong, MP Tornai. “Pilot patient studies using a dedicated dual-modality SPECT-CT system for breast imaging.” Presented at the *2008 American Association of Physicists in Medicine Meeting*, Houston, TX, 27-31 Jul. 2008, and published in Med. Phys. 35(6): 2894.

KL Perez, SJ Cutler, P Madhav, MP Tornai “Towards Quantification of Dedicated Breast SPECT Using Non-Traditional Acquisition Trajectories.” Presented at the *2009 Duke Cancer Center Annual Meeting*, Durham, NC, 05 Oct. 2009.

P Madhav, DJ Crotty, SJ Cutler, **KL Perez**, MP Tornai. “3D Molecular Breast Imaging Using Dedicated SPECT-CT.” Presented at the *2009 Breast Imaging Scientific Symposium*, Chapel Hill, NC, 29 Oct. 2009.

E. Conclusions

In Year 3, progress was made for Task 1 and Task 3(b). The robustness of the procedure for quantifying radioactive uptake in the breast was evaluated. The TOST statistical analysis for equivalence was used to compare the activity concentration measured in the reconstructed SPECT image with known value measured in a dose calibrator. The next steps for this project will be to collect breast images from human subjects who have already been injected with the ^{99m}Tc-sestamibi radiotracer to quantify the range of activity concentration in otherwise normal tissue. A major effort in Year 3 has been writing and preparing to defend my dissertation.

F. References

[1] M. K. O'Connor, S. W. Phillips, C. B. Hruska, D. J. Rhodes, and D. A. Collins, "Molecular Breast Imaging: Advantages and Limitations of a Scintimammographic Technique in Patients with Small Breast Tumors," *The Breast Journal,* vol. 13, pp. 3-11, 2007.

[2] C. N. Archer, M. P. Tornai, J. E. Bowsher, S. D. Metzler, B. C. Pieper, and R. J. Jaszczak, "Implementation and initial characterization of acquisition orbits with a dedicated emission mammotomograph," *IEEE Trans. Nucl. Sci.*, vol. 50, p. 413, 2003.

[3] R. J. Jaszczak, K. L. Greer, C. E. Floyd, Jr., C. C. Harris, and R. E. Coleman, "Improved SPECT Quantification Using Compensation for Scattered Photons," *J Nucl Med,* vol. 25, pp. 893-900, August 1, 1984 1984.

[4] K. L. Perez, S. J. Cutler, P. Madhav, and M. P. Tornai, "Towards quantification of dedicated breast SPECT using non-traditional acquisition trajectories," in *Nuclear Science Symposium Conference Record (NSS/MIC), 2009 IEEE*, 2009, pp. 3866-3870.

[5] J. E. Bowsher, V. E. Johnson, T. G. Turkington, R. J. Jaszczak, C. R. Floyd, and R. E. Coleman, "Bayesian reconstruction and use of anatomical a priori information for emission tomography," *IEEE Trans Med Imaging,* vol. 15, pp. 673-86, 1996.

[6] K. L. Perez, S. J. Cutler, P. Madhav, and M. P. Tornai, "Characterizing the contribution of cardiac and hepatic uptake in dedicated breast SPECT using tilted trajectories," *Physics in Medicine and Biology,* vol. 55, pp. 4721-4734, Aug 21 2010.

APPENDIX A: STATEMENT OF WORK

Task 1 Acquire IRB approval to conduct SPECT patient studies and image planar needles (Months 1-6)

a. Participate on writing IRB protocol for FMT imaging in a high risk patient cohort. (Month 1)
b. Modify rpFNA IRB protocol (PI: Seewaldt #4245) to include imaging of planar needles extracted from patient breasts. (Month 1)

Task 2 Evaluate radioactive needles for guided histology (Months 1-36)

a. Design shielded holder or sleeves to image the individual signal from each biopsy needle. (Months 1-3)
b. Construct holder. (Month 4)
c. Use phantoms to test designed holder, and modify as necessary. (Month 5)
d. Obtain 2D image of biopsy needles. (Month 6-36)
e. Analyze the 2D images to determine which needles should be histologically evaluated. (Months 6-36)
f. Determine if there is a statistical correlation between the histology results and the 2D molecular images. (Months 6-36)

Task 3 Optimize patient imaging and biopsy protocol (Months 1-36)

a. Investigate how the dedicated SPECT imaging and biopsy procedures can be optimally integrated to minimize the patient scan times. (Month 1-3)
b. Investigate how the information gained with SPECT imaging can be incorporated into the biopsy procedure. (Months 1-3)
c. Image patients. (Months 6-36)
d. Analyze SPECT studies of returning patients to determine variability in patient setup and image acquisitions. (Months 12-36)

Task 4 Complete other aspects of breast cancer training program (Months 1-36)

a. Shadow a radiologist(s) to observe clinical and diagnostic side in breast cancer imaging (Nuclear Medicine, Mammography). (Months 1-12)
b. Publish research work in peer-reviewed journals. (Months 1-36)
c. Attend and present at local seminars offered at Duke University through Medical Physics and the Breast and Ovarian Oncology Research Program, which is part of the Duke Comprehensive Cancer Center. (Months 1-36)
d. Attend international conferences such as DOD BCRP Era of Hope Meeting, IEEE Medical Imaging Conference, RSNA Conference, Society of Nuclear Medicine or San Antonio Breast Cancer Symposium. (Months 1-36)
e. Prepare and defend thesis. (Months 30-36)

APPENDIX B: CONFERENCE PROCEEDING

Is SPECT or CT Based Attenuation Correction More Quantitatively Accurate for Dedicated Breast SPECT Acquired with Non-Traditional Trajectories?

Kristy L. Perez, *Student Member*, Steve D. Mann, *Student Member*, Jan H. Pachon, *Student Member*, Priti Madhav, *Student Member*, Martin P. Tornai, *Senior Member*

***Abstract*- Attenuation correction is necessary for SPECT quantification. There are a variety of methods to create attenuation maps. For dedicated breast SPECT-CT imaging, it is unclear if either a SPECT- or CT-based attenuation map would provide the most accurate quantification and whether or not segmenting the different tissue types will have an effect on the quantification. For these experiments, ^{99m}Tc diluted in methanol and water filled geometric and anthropomorphic breast phantoms was imaged with a dedicated dual-modality SPECT-CT breast scanner. SPECT images were collected using a compact CZT camera with various 3D acquisition trajectories including vertical and 30° tilted parallel beam, and complex sinusoidal trajectories. CT images were acquired using a quasi-monochromatic x-ray source and CsI(T1) digital flat panel detector in a half-cone beam geometry. Measured scatter correction for SPECT and CT were implemented. To compare photon attenuation correction in the reconstructed SPECT images, various volumetric attenuation maps were derived from 1) uniform SPECT, 2) uniform CT, and 3) segmented CT, populated with different attenuation coefficient values. Comparisons between attenuation masks using phantoms consisting of materials with different attenuation values show that at 140 keV the differences in the attenuation between materials do not affect the quantification as much as the size and alignment of the attenuation map. The CT-based attenuation maps give quantitative values 30% below the actual value, but are consistent. The SPECT-based attenuation maps can provide within 10% accurate quantitative values, but are less consistent.**

I. Introduction

A variety of physical factors affect the quantification of single photon emission computed tomography (SPECT) images [1]. Additionally, image artifacts arise from physical processes and sampling, especially with systems capable of 3D acquisition trajectories, which can yield an incorrect absolute activity of the tracer. Photon attenuation in the body impairs image quantification by reducing the total number of counts detected by the SPECT camera. Attenuation correction relies on obtaining a spatial distribution of attenuation coefficients to model the imaged object and compensates for non-uniform attenuation. For some imaging tasks, assuming a constant attenuation distribution can be sufficient [2]. However, this distribution can also be derived more accurately from computed tomography (CT) data.

Using CT-based attenuation correction must account for a variety of factors pertaining to the differences in the SPECT and CT modalities, such as different resolutions, imaging (and attenuation) energies, and, for our system in particular, different imaged volumes and orientations. The differences in resolution and alignment have been shown to be problematic when using a CT image to correct SPECT studies. Misregistration of 2 to 3 cm has been shown to cause a 20 to 35% change in radiotracer distribution [3]. Another study found that a 7 mm misalignment caused a 15% change in apparent radiotracer uptake [4]. These errors can be introduced by the registration software or by the user variability interacting with registration software [5]. Using the SPECT reconstruction does not introduce these errors, and may be an appropriate method considering the nearly uniform attenuation of varying breast tissues at 140 keV.

In this study, attenuation maps based on reconstructed SPECT and CT data are compared. CT-based attenuation maps were created both by linearly scaling the attenuation coefficients measured at 36 keV to 140 keV as well as filling in the known attenuation coefficient at 140 keV. The CT-based attenuation maps created were used to apply one correction/value to the data, as well as segmented the data and then applied the corrections/values for water and methanol separately. The effect of the different SPECT acquisition trajectories was also observed.

II. Methods

A. Gamma Camera and Data Acquisition

The SPECT sub-system of the hybrid imaging device consists of a Cadmium-Zinc-Telluride (CZT) *LumaGEM* 3200S^{TM} gamma camera (*Gamma Medica Inc.*, Northridge, CA) that has 2.5x2.5 mm^2 pixels and a sensitivity of 37.9 cps/MBq (Fig. 1). The lead parallel hole collimator has 1.22 mm flat-to-flat hexagonal holes with 0.2 mm septa and is 25.4 mm in height. The camera system is attached to precision positioning motors to permit movement in 3D to contour the breast surface by moving in and out, up and down and around the center of rotation. Previous work has defined a set of trajectories which maximize the volume of the object imaged [6].

The CT sub-system has a rotating tungsten target x-ray source (*Rad-94, Varian Medical Systems*, Salt Lake City, UT), with a 0.4 focal size and 14° anode angle, and a 20x25 cm^2 CsI(T1)-based amorphous silicon digital x-ray detector (*Paxscan 2520, Varian Medical Systems*, Salt Lake City, UT) with a grid size of 1920x1536 pixels on a 127 µm pitch (Fig. 1). The x-ray source and detector are attached to U-shaped

Manuscript received November 9, 2010. This work has been funded by the National Cancer Institute of the National Institutes of Health (R01-CA096821, T32-EB001040, and T32EB007185) and the Department of Defense Breast Cancer Research Program (W81XWH-08-1-0192).

KLP, SDM, JHP and MPT are with the Medical Physics Program and Radiology Department, Duke University, Durham, NC 27710 USA (telephone: 919-684-7943, e-mail: kristy.perez@duke.edu).

JHP, PM and MPT are with Biomedical Engineering and Radiology Departments, Duke University, Durham, NC 27710 USA.

PM is currently with *GE Healthcare*, Waukesha, WI.

metal plate securing the two at a fixed tilt and are adjoined to a common azimuthal rotation stage (model RV350CCHL, *Newport Corp.*, Irvine, CA). The collimator attached to the x-ray source holds a cerium 100th attenuating value layer (0.0508cm) filter (Z=58, ρ=6.77g/cm^3, K-edge=40.4keV, *Santoku America, Inc.*, Tolleson, AZ), which yields a mean beam energy of ~36 keV and FWHM of 15% [7].

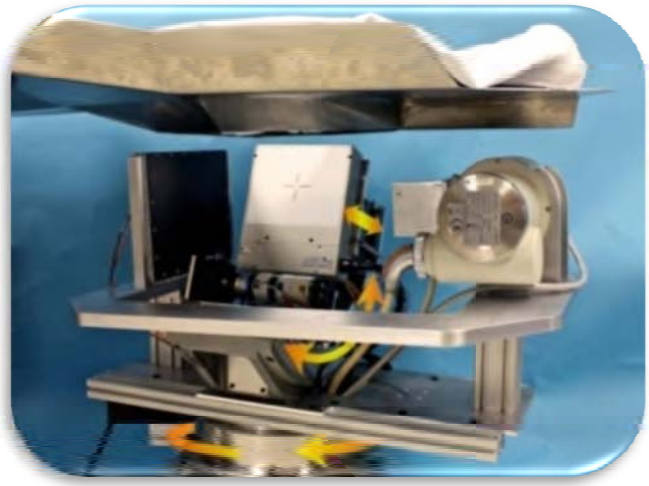

Fig. 1. Hybrid SPECT-CT breast imaging device. Orange and yellow arrows indicate the directions of movement of the SPECT camera (center). X-ray source (right) and detector (left) orbit the center-of-rotation at a fixed tilt.

B. Geometric & Anthropomorphic Phantoms

1) Cylindrical Phantom

The cylindrical phantom consisted of 4 syringes filled with ^{99m}Tc-pertechnetate diluted in 10 mL of methanol (ρ = 0.78 g/cm^3) or water (ρ = 1.0 g/cm^3) in order to vary the density of the attenuating material. The initial radioactive concentrations, measured with a calibrated dose calibrator (CRC-30BC, *Capintec, Inc*., Ramsey, NJ), are given in Table I. The syringes were placed in a 12.5 cm diameter cylinder (Fig. 2) filled with aqueous ^{99m}Tc-pertechnetate. Additionally, four 6 mm diameter nylon spheres that had been soaked in 1 mCi of ^{99m}Tc-pertechnetate for ~1 hour were taped to the outside of the cylinder. Due to the opposite charges of the pertechnetate and nylon, the radioactive molecule collects on the surface of the sphere and is used as a fiducial marker to register SPECT and CT images.

TABLE I: INITIAL ACTIVITY CONCENTRATION IN SYRINGES AND SYRINGE-TO-BACKGROUND RATIO IN CYLINDER.

	Activity Concentration (uCi/mL)	**Syringe:Bkgd Ratio**
Methanol High	33.6	8:1
Methanol Low	16.0	4:1
Water High	32.3	8:1
Water Low	16.9	4:1

2) Breast & Lesion Phantoms

A 700 mL anthropomorphic breast phantom contained two 5.4 mL acrylic-walled spherical lesions (*Radiological Support Devices Inc.*, Newport Beach, CA), one filled with ^{99m}Tc pertechnetate diluted into methanol and the other with ^{99m}Tc pertechnetate diluted into water (Fig. 3). Table II gives the initial radioactive concentrations, measured with a dose calibrator, of the spheres and background. Additionally, four 6 mm diameter, ^{99m}Tc-pertechnetate soaked, nylon spheres were taped to the outside of the breast phantom to aid in image registration.

Fig. 2. Photograph of syringes with varying concentrations of radioactivity in a cylinder with an aqueous uniform radioactive background. Green syringes are filled with methanol, and purple syringes are filled with water. Medical tape attached to outside of the container secure fiducial markers used to register SPECT and CT images.

TABLE II: INITIAL ACTIVITY CONCENTRATION OF THE LESIONS IN THE BREAST PHANTOM AND THE LESION-TO-BACKGROUND RATIO.

	Activity Concentration (uCi/mL)	**Lesion:Bkgd Ratio**
Methanol	26.2	7:1
Water	27.0	7:1

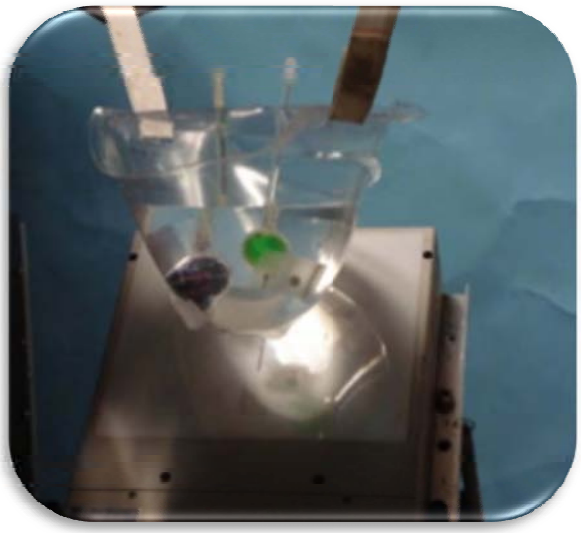

Fig. 3. Photograph of the water-filled (purple) and methanol-filled (green) spheres in the suspended anthropomorphic breast phantom filled with 700 mL of water. Medical tape attached to outside of the breast secures fiducial markers used to register SPECT and CT images.

C. Data Acquisition

For this data, 128 projection images collected over 360º with vertical axis of rotation (VAOR), 30º tilted parallel beam (TPB), and sinusoidal wave projected onto a hemisphere ranging from 15º to 45º polar tilt (PROJSINE) trajectories (Fig. 4) were compared for quantification accuracy. The data was collected with a ±4% photopeak energy window centered about 140 keV.

Fig. 4. Rendering of the 3D trajectories (yellow path) of the gamma camera (blue box) used to acquire data of the cylinder and breast phantoms.

Additionally, 240 x-ray projection images acquired with 60 kVp and 1.25 mAs were collected both without and with a lead-bead scatter grid in place, such that the projections could be scatter corrected prior to reconstruction, resulting in nearly absolute attenuation coefficients [8].

D. Creating Attenuation Maps & Reconstructing Data

SPECT image reconstruction was performed using a ray-driven, iterative ordered-subsets expectation maximization (OSEM) reconstruction code [9]. CT image reconstruction used an OSC iterative reconstruction code [10, 11].

For SPECT based attenuation correction, a map of the attenuation coefficients was defined by reconstructing the data to the first iteration, thresholding the image to obtain the mask of the object, and assigning each pixel a constant attenuation coefficient for water, 0.1545 cm^{-1} at 140 keV (Fig. 5, TOP). The scatter corrected, reconstructed CT images used for attenuation correction were either: 1) filled with a constant attenuation coefficient of water, 0.1545 cm^{-1}; 2) segmented into two components and filled with attenuation coefficients of water, 0.1545 cm^{-1}, and methanol, 0.1234 cm^{-1}; 3) scaled linearly based on the attenuation coefficient of water from 36 keV to 140 keV; and 4) segmented water and methanol attenuation coefficients and linearly scaled them from 36 keV to 140 keV (Fig. 5).

The original emission data was reconstructed implementing each of the five attenuation maps as well as the collimator, geometry and detection efficiencies of the SPECT camera, radiopharmaceutical half-life, and scatter correction maps in the reconstruction algorithm as previously described [12]. The data was reconstructed to the 20^{th} iteration, near convergence. A reconstruction grid size of 150x150x150 was used. The isotropic voxel size was selected to be the same as the detector pixel size, with 2.5 mm on each side. Thus, gray scale values of the reconstructed images are output in absolute µCi/mL units.

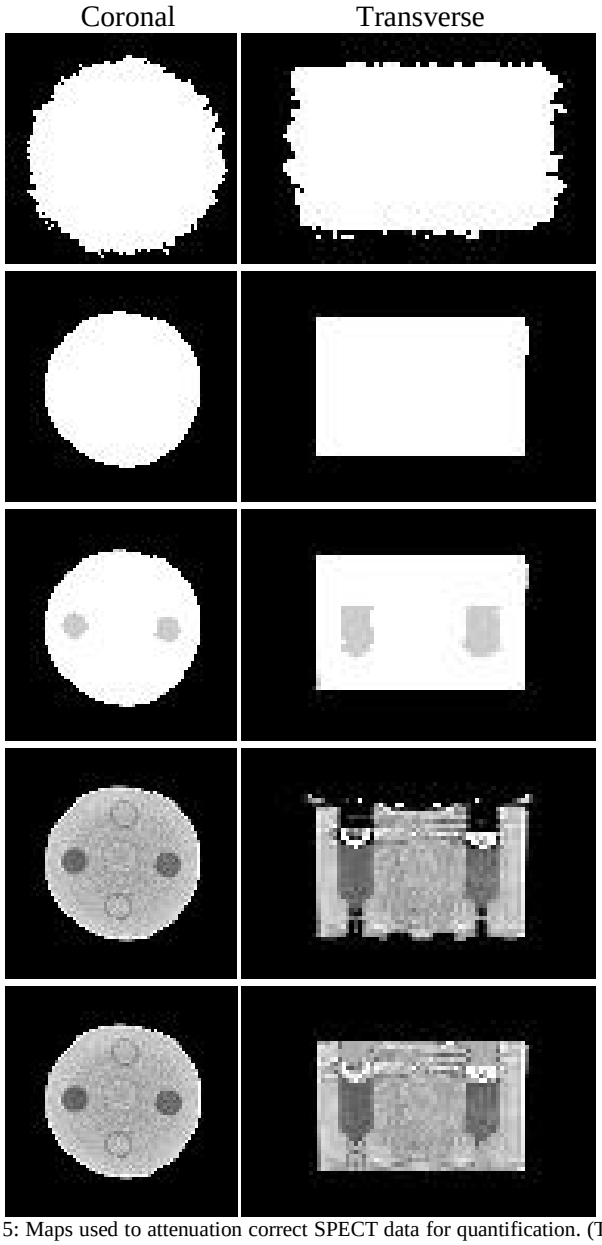

Fig. 5: Maps used to attenuation correct SPECT data for quantification. (TOP to BOTTOM) 1) SPECT-based attenuation map and 2) CT-based attenuation maps with constant value of water, 3) segmented CT with constant values of water and methanol, 4) CT-based water attenuation coefficient linearly scaled from 36 to 140 keV, and 5) CT-based, segmented water and methanol attenuation coefficients linearly scaled from 36 to 140 keV.

E. Data Analysis

Volumes of interest (VOIs) for the syringes were completely within and not close to the edges of the syringes to avoid partial volume edge effects. The mean, decay corrected, reconstructed image activity concentration was determined and compared with the dose calibrator measured activity concentration. The percent difference was calculated to determine the accuracy of the reconstruction process.

III. Results

A. Cylinder Phantom

There were no obvious qualitative differences in the SPECT images reconstructed with the different attenuation maps (Fig. 6). However, it was noted that if CT-based attenuation maps are not correctly aligned with respect to where the SPECT

reconstruction code places the image within the matrix, artifacts and quantitative inaccuracies will result.

Quantitatively, the SPECT-based attenuation correction was more accurate than the CT-based attenuation corrections (Fig. 7). However, the CT-based attenuation corrections produced more consistent results of approximately 73% of the known value.

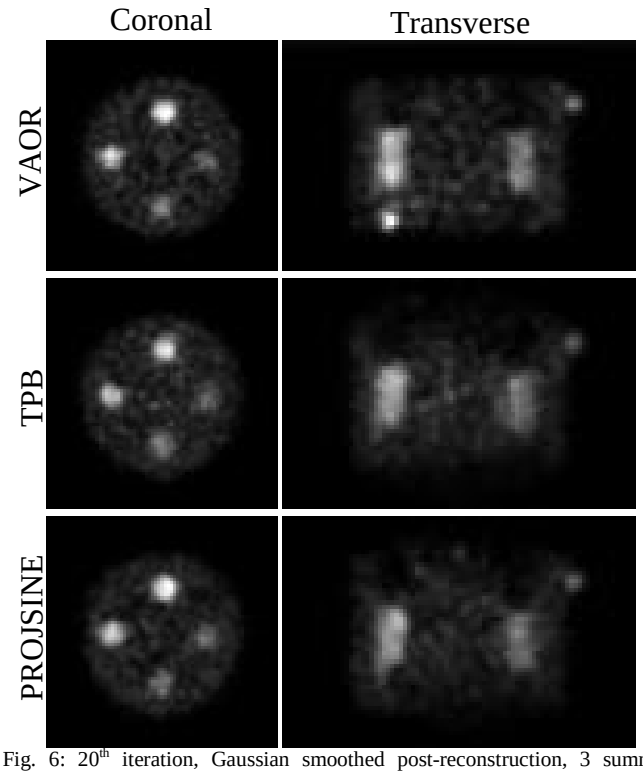

Fig. 6: 20th iteration, Gaussian smoothed post-reconstruction, 3 summed reconstructed slices of the cylinder and syringes in the (LEFT) coronal and (RIGHT) transverse planes. Images are SPECT-based attenuation corrected collected with the indicated trajectories.

B. Breast & Lesion Phantoms

The reconstructed images for each trajectory about the lesion-containing breast phantom with each attenaution map are very similar (Fig. 8). The SPECT-based attenuation corrected mean activity concentration has good agreement with "known" values, while CT-based attenaution corrections are less accurate, but similarly consistent (Fig. 9) as with the cylinders.

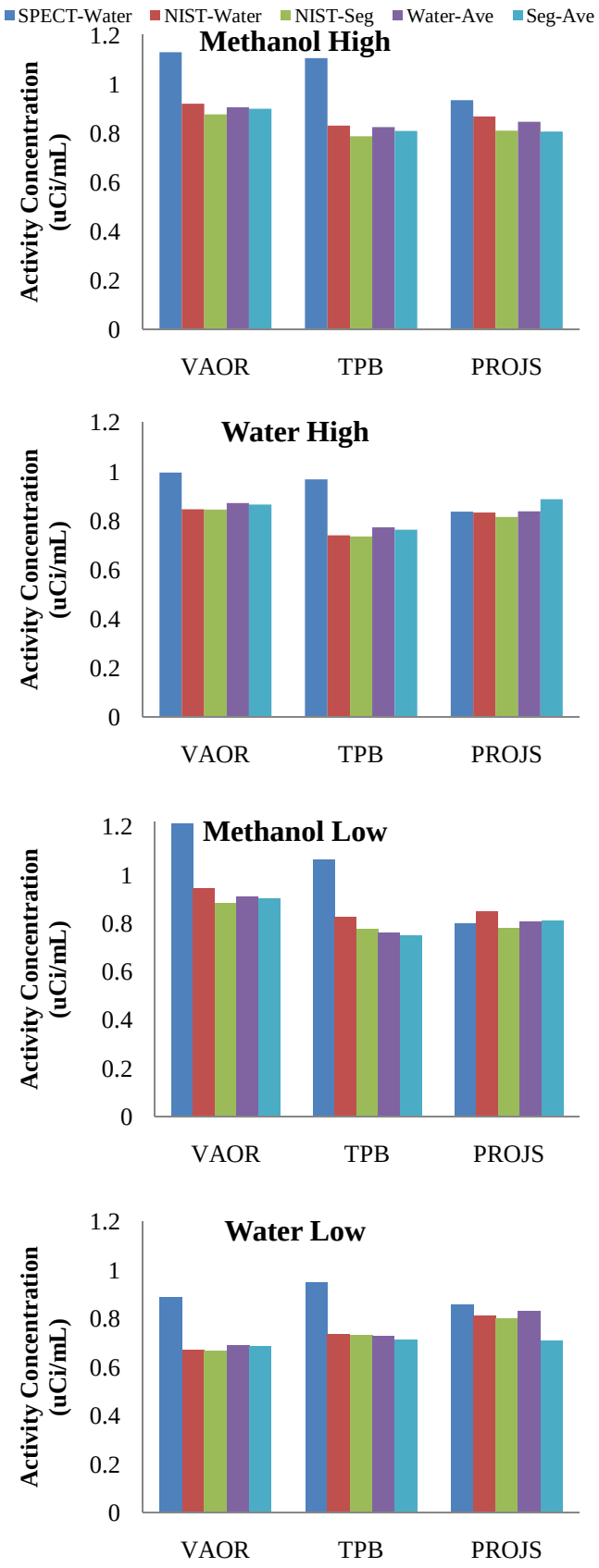

Fig. 7. Bar charts of the ratio of image measured activity concentration to the dose calibrator known activity concentration of each syringe for each attenuation map and each SPECT acquisition trajectory. A ratio = 1 indicates the perfect image quantification.

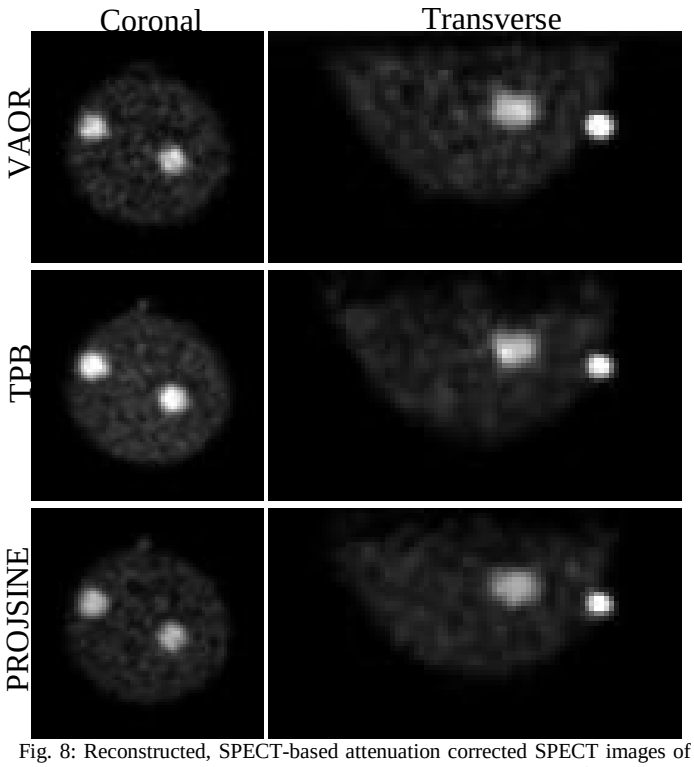

Fig. 8: Reconstructed, SPECT-based attenuation corrected SPECT images of the breast with methanol (right in coronal image) and water (left in coronal image) lesions collected with trajectories as indicated. The dot outside the breast seen in the transverse images is one of the fiducial markers.

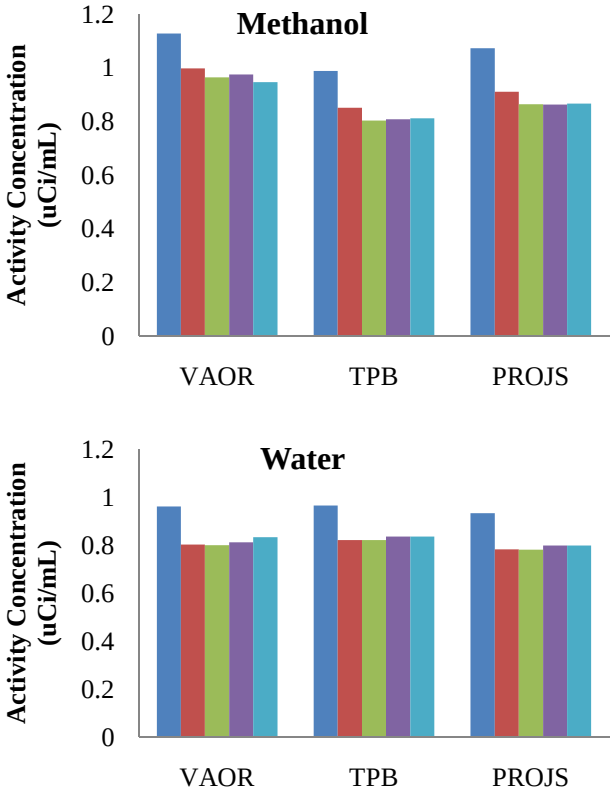

Fig. 9. Bar charts of the ratio image measured activity concentration to the dose calibrator known activity concentration of each lesion for each attenuation map and each SPECT acquisition trajectory. A ratio = 1 indicates the best quantification.

IV. Disscussion

In this study, the SPECT-based attenuation map yielded better accuracy than the CT-based attenuation corrections, but the CT-based maps produce more consistent and precise results. One potential reason for the less accurate CT-based correction is that the quantification method was first developed with the SPECT-based attenuation map, and thus maybe biased towards it. Nonetheless, the CT-based attenuation correction quantification data implies that accounting for the difference in attenuation coefficients at 140 keV of water (0.1545 cm^{-1}) and methanol (0.1234 cm^{-1}) does not make a difference in the quantitative accuracy. The CT-based attenuation maps were slightly more accurate when using the water only attenuation coefficient even when quantifying the activity concentration of methanol syringe/lesion. Therefore, it seems feasible to either use a uniform SPECT-based attenuation map or scale the CT data with a constant linear scaling term in the future.

The CT-based attenuation maps are consistently between 20 to 35% lower than the known activity concentration, similar to previous results seen in our lab, where the known absolute volume was used to quantify SPECT images [13]. Since the CT-based attenuation correction appears more consistently reproducible, it may be more clinically useful after scaling adjustments accounting for volume mismatch. Alternatively, if resolution recovery was employed in the SPECT reconstruction, perhaps the reduced blur and more accurate volumes in the SPECT images coupled with the CT images would produce more accurate and reproducible quantification. This is a topic to be explored in future research.

It should be noted that VOI placement can affect the apparent accuracy of quantification. For this data set, large VOIs completely within the object of interest were selected to minimize partial volume sampling. However, changing the VOI placement could report different mean image values, but not different trends.

Images were registered using *AMIDE* software, where the uncertainty of registration is on the order of 2 to 3mm/point, based on the potential for mis-identifying the center of a fiducial marker. Given that it has been shown elsewhere that a 7mm shift can cause up to 15% inaccuracy in radioactivity distribution [4], this mis-alignment could reduce the accuracy of quantification when the CT-based attenuation maps are used. Additional alignment errors could be introduced when writing out rotated (interpolated) images in *AMIDE*, introducing potential manual alignment errors, especially at the edge of the object or at interfaces between segmented volumes (e.g. methanol and water). One caveat was that we did not segment the plastic components of the phantom in this study. Further investigation into more accurate image registration software should be done to reduce these issues.

V. Conclusions

A method to quantify the activity concentration of regions of interest in data acquired with our unique dedicated SPECT-CT system was implemented. The SPECT-based attenuation map currently provides the most accurate quantification, but the

CT-based attenuation correction provides the most precise. With better registration, the CT-based assessment could be improved and provide more consistent results.

V. Acknowledgements

MPT is an inventor of this dedicated SPECT-CT imaging technology, and is named as an inventor on the patent for this technology assigned to Duke. If this technology becomes commercially successful, MPT and Duke could benefit financially.

References

[1] M. S. Rosenthal, J. Cullom, W. Hawkins, S. C. Moore, B. M. Tsui, and M. Yester, "Quantitative SPECT imaging: a review and recommendations by the Focus Committee of the Society of Nuclear Medicine Computer and Instrumentation Council," *J Nucl Med*, vol. 36, pp. 1489-513, Aug 1995.

[2] S. R. Cherry, J. A. Sorenson, and M. E. Phelps, *Physics in Nuclear Medicine, 3rd ed* vol. 234. Philadelphia, PA: Saunders, 2003.

[3] C. D. Stone, J. W. McCormick, D. R. Gilland, K. L. Greer, R. E. Coleman, and R. J. Jaszczak, "Effect of Registration Errors Between Transmission and Emission Scans on a SPECT System Using Sequential Scanning," *J Nucl Med*, vol. 39, pp. 365-373, February 1, 1998 1998.

[4] Y. Takahashi, K. Murase, H. Higashino, T. Mochizuki, and N. Motomura, "Attenuation correction of myocardial SPECT images with X-ray CT: Effects of registration errors between X-ray CT and SPECT," *Annals of Nuclear Medicine*, vol. 16, pp. 431-435, 2002.

[5] S. Goetze, T. L. Brown, W. C. Lavely, Z. Zhang, and F. M. Bengel, "Attenuation Correction in Myocardial Perfusion SPECT/CT: Effects of Misregistration and Value of Reregistration," *J Nucl Med*, vol. 48, pp. 1090-1095, July 1, 2007 2007.

[6] C. N. Brzymialkiewicz, M. P. Tornai, R. L. McKinley, and J. E. Bowsher, "Evaluation of fully 3-D emission mammotomography with a compact cadmium zinc telluride detector," *Medical Imaging, IEEE Transactions on*, vol. 24, pp. 868-877, 2005.

[7] R. L. McKinley, M. P. Tornai, E. Samei, and M. L. Bradshaw, "Initial study of quasi-monochromatic beam performance for x-ray computed mammotomography," *IEEE Trans. Nucl. Sci.*, vol. 52, pp. 1243-1250, 2005.

[8] P. Madhav, C. M. Li, and M. P. Tornai, "Development of in vivo characterization of breast tissues through absolute attenuation coefficients using dedicated cone-beam CT," in *Medical Imaging 2010: Physics of Medical Imaging*, San Diego, California, USA, pp. 762209-11.

[9] J. E. Bowsher, M. P. Tornai, S. D. Metzler, J. Peter, and R. J. Jaszczak, "SPECT breast imaging using more nearly complete orbits and combined pinhole-parallel-beam collimation," in *Nuclear Science Symposium Conference Record, 2001 IEEE*, 2001, pp. 1328-1330 vol.3.

[10] F. J. Beekman and C. Kamphuis, "Ordered subset reconstruction algorithm for x-ray CT," *Phys Med Biol*, vol. 46, 2001.

[11] J. S. Kole and F. J. Beekman, "Evaluation of the ordered subset convex algorithm for cone-beam CT," *Phys Med Biol*, vol. 50, 2005.

[12] K. L. Perez, S. J. Cutler, P. Madhav, and M. P. Tornai, "Towards quantification of dedicated breast SPECT using non-traditional acquisition trajectories," in *Nuclear Science Symposium Conference Record (NSS/MIC), 2009 IEEE*, 2009, pp. 3866-3870.

[13] S. J. Cutler, "Evaluation of a Dedicated SPECT-CT Mammotomography System for Quantitative Hybrid Breast Imaging," in *Biomedical Engineering*. vol. PhD Durham: Duke University, 2010.